



Science Arts & Métiers (SAM)

is an open access repository that collects the work of Arts et Métiers Institute of Technology researchers and makes it freely available over the web where possible.

This is an author-deposited version published in: <https://sam.ensam.eu>
Handle ID: <http://hdl.handle.net/10985/17879>

To cite this version :

C. MANCINI, Mirko FARANO, Pietro DE PALMA, Stefania CHERUBINI, Jean-Christophe ROBINET - Global stability analysis of lifted diffusion flames - Energy Procedia - Vol. 126, p.867-874 - 2017

Any correspondence concerning this service should be sent to the repository

Administrator : scienceouverte@ensam.eu



72nd Conference of the Italian Thermal Machines Engineering Association, ATI2017, 6–8
September 2017, Lecce, Italy

Global stability analysis of lifted diffusion flames

C. Mancini^a, M. Farano^{a,b}, P. De Palma^{a,*}, J. C. Robinet^a, S. Cherubini^a

^a*DMMM, Politecnico di Bari, Via Re David 200, 70125 Bari, Italy*

^b*DynFluid Laboratory, Arts et Metiers ParisTech, 151 Boulevard de l'Hopital, 75013 Paris, France*

Abstract

This work describes the development of a method for the global hydrodynamic stability analysis of diffusion flames. The low-Mach-number (LMN) Navier–Stokes (NS) equations for reacting flows are solved together with a transport equation for the mixture fraction describing the local composition of the fluid. The equations are solved by the spectral-element code NEK5000 with Legendre polynomial reconstruction of degree twelve and second-order accurate Runge-Kutta time integration scheme. In order to compute the base flow for the stability analysis, a selective frequency damping approach has been employed. The global stability analysis has been performed by a matrix-free time-stepper algorithm applied to the LMN-NS equations, using an Arnoldi method to compute the most unstable modes. Moreover, a numerical linearization of the governing equation is employed, which allows one to study the stability of diffusion flames without the direct evaluation and storage of the linearized operator. Therefore, a remarkable reduction of the storage capacity is achieved and a more flexible numerical approach is obtained. The numerical model has been validated by comparison with the results for the axisymmetric diffusion flame available in the literature.

Peer-review under responsibility of the scientific committee of the 72nd Conference of the Italian Thermal Machines Engineering Association

Keywords: hydrodynamic stability; time-stepper approach; low Mach number; unstable modes.

1. Introduction

Lifted flames are common in many engineering applications such as gas-turbine combustion chambers, burners, and rocket engines. The flame does not anchor to the injector rim when the flame propagation velocity in the upstream direction equals the flow velocity at some distance from the inlet plane. The flame velocity depends on the characteristics of the fuel and of the oxidizer and on their mixing process. In most gas-turbine combustion chambers, the lifting distance depends also on the inlet flow swirl, which creates a recirculation region downstream of the injector, anchoring the flame [1].

In the present work a non-swirling jet diffusion flame is considered. Such a flame has a typical triple-flame structure with a lean branch and a rich branch in the base premixed region, which anchor the diffusion part of the flame extending downstream along the stoichiometric surface.

* Corresponding author. Tel.: +39-080-5963226 ; fax: +39-080-5963411.
E-mail address: pietro.depalma@poliba.it

The hydrodynamic stability of a jet diffusion flame has been recently studied by using local [2] and global [1] stability analysis, considering an axisymmetric jet of fuel issuing in a large cylindrical domain.

A pocket of absolute instability [2] at the injector exit (wavemaker) produces oscillations which are convected and amplified downstream. The hydrodynamic stability properties of the flow upstream of the flame base is different from that downstream of it. The upstream part is more unstable and can influence the behavior of the entire flow [1]. These instabilities may become dangerous when coupled with thermo-acoustic perturbations. For small lift-off height, for example in H_2/O_2 rocket engines where the flame speed is very high, the pocket of absolute instability reduces and does not support unstable global modes, so that the entire flow may stabilize.

Nichols (2008) et al. have shown that two peak-frequency ranges for the oscillations exist: a high frequency range, $0.25 < St < 0.3$, and a low frequency range, $St < 0.05$, St being the Strouhal number. They showed that the high-frequency oscillations are linked to the absolutely unstable premixing region, whereas they postulated that the low-frequency oscillations were due to nonlinear interactions among resonant modes.

The local stability analysis is not fully suited for this kind of application since the heat release modifies sharply the stability properties of the flow. For this reason, Qadri et al. (2015), performed a global stability analysis using the same test case. They have shown that two families of global mode exist, called mode A and B. Mode A is linked to high-frequency oscillations and its wavemaker is located in the shear layer in the premixing region. Mode B has global frequency close to the low-frequency oscillations computed by [2], and its wavemaker is located in the outer part of the shear layer of the flame.

The approach employed by Qadri is based on a linearization of the differential operator governing the phenomenon. and on the time-stepper approach proposed in references [3, 4] to compute the eigenpairs of the exponential propagator. Such an approach allows one to avoid the explicit storage of the linearized operator and a direct computation of its eigenvalues; this is needed especially for computations in three space dimensions, where the number of degrees of freedom can be too large.

In the present work, we employ a time-stepper approach and also avoid the linearization procedure by adopting a numerical evaluation of the eigenpairs of the exponential propagator. In this way, we provide a more flexible approach, which can be applied straightforwardly to any complex system of conservation equations governing the dynamics of a reacting flow. Such a method is validated versus the results of Qadri et al. (2015) using the same test case proposed by Nichols et al. (2008).

2. Problem formulation

The present work provides the hydrodynamic stability analysis of a jet diffusion flame. The concentration of fuel and oxidizer is described using the mixture fraction parameter (see [5]), $Z = \frac{sY_{fuel} - Y_{ox} + Y_{ox}^0}{sY_{fuel}^0 + Y_{ox}^0}$, where Y indicates concentrations of fuel and oxidizer while Y^0 indicates the corresponding inlet values and s is the reaction stoichiometric ratio so that $Z = 1$ for pure fuel and $Z = 0$ for pure oxidizer.

Following the approach of [2], we use the low-Mach-number Navier–Stokes (LMN-NS) equations with a closing equation to link density, ρ , temperature, T , and mixture fraction:

$$\frac{\partial \rho}{\partial t} + \nabla \cdot (\rho \mathbf{u}) = 0, \quad (1)$$

$$\rho \left(\frac{\partial \mathbf{u}}{\partial t} + \mathbf{u} \cdot \nabla \mathbf{u} \right) = -\nabla p + \nabla \cdot \left(\frac{\tau}{S_1 Re} \right), \quad (2)$$

$$\rho \left(\frac{\partial Z}{\partial t} + \mathbf{u} \cdot \nabla Z \right) = \frac{\nabla^2 Z}{S_1 Re Sc}, \quad (3)$$

$$\rho \left(\frac{\partial T}{\partial t} + \mathbf{u} \cdot \nabla T \right) = \frac{\nabla^2 T}{S_1 Re Sc} + Da \rho^3 \omega, \quad (4)$$

$$\rho[(S_1 - 1)Z + 1][(S_2 - 1)T + 1] = 1, \quad (5)$$

where p indicates the pressure, \mathbf{u} is the velocity vector, and $\tau = [\nabla \mathbf{u} + (\nabla \mathbf{u})^T] - 2/3(\nabla \cdot \mathbf{u})\mathbf{I}$. The flow variables have been non-dimensionalized by the jet diameter at inlet, d , inlet fuel jet velocity, u_j , and oxidizer density, ρ_o . The non-dimensional temperature is $T = \frac{T^* - T_0}{T_f - T_0}$, where T^* is the dimensional temperature [K], T_f is the dimensional adiabatic flame temperature [K] and T_0 is the dimensional ambient oxidizer temperature [K]. S_1 represents the ratio of the oxidizer density to the fuel density, ρ_j ; whereas, S_2 is the the ratio of the adiabatic flame temperature to the oxidizer temperature. In equation (4) the source term, $Da\rho^3\omega$, is the non-dimensional rate of enthalpy release per unit volume. In particular, a simple Arrhenius law has been used for the reaction rate,

$$\omega = \left[\left(Z - \frac{T}{s+1} \right) \left(1 - Z - \frac{sT}{s+1} \right) - \kappa T^2 \right] e^{\left(\frac{-\beta(1-T)}{1-\alpha(1-T)} \right)}, \quad (6)$$

that includes the following chemistry parameters: the equilibrium constant κ ; the mass stoichiometric ratio s ; the heat release parameter $\alpha = (T_f - T_0)/T_f$; the Zeldovich number, $\beta = \alpha T_a/T_f$, where T_a is the dimensional activation temperature of the considered reaction. Re , Pr and Sc indicate the Reynolds, Prandtl and Schmidt numbers, respectively. Finally, Da is the Damköhler number, $Da = (1+s) \frac{\Delta h}{c_p(T_f - T_0)} \frac{A d}{u_j}$, where Δh is the enthalpy change due to combustion, c_p the specific heat at constant pressure and A the pre-exponential factor. This parameter is very important in this case of study: it specifies the ratio of the rate of reaction to the rate of fluid convection and controls the transition from stable to unstable flame.

2.1. Global stability analysis

Linear stability analysis allows one to investigate the asymptotic time evolution of global infinitesimal perturbations in the vicinity of a given fixed point of the governing equations. We recast these equation in the following compact form, $\frac{\partial \mathbf{q}}{\partial t} = \mathcal{N}(\mathbf{q})$, where $\mathbf{q} = (u_x, u_r, Z, T)^T$ and \mathcal{N} is the nonlinear partial differential operator (the density is not included since it can be derived from the mixture fraction and the temperature by using equation (5)). The dynamics of an infinitesimal perturbation $\mathbf{q}'(x, r, t)$ is governed by the following linearized equation (with respect to a given base point \mathbf{q}_b): $\frac{\partial \mathbf{q}'}{\partial t} = \mathcal{L}(\mathbf{q}')$, where \mathcal{L} is a suitable linearized operator. Since, especially for computations in three space dimensions, the number of degrees of freedom can be too large to enable explicit storage of matrix \mathcal{L} and a direct computation of its eigenvalues, the time-stepper approach proposed by Edwards et al. (1994) and Bagheri et al. (2009a) is here employed. Given an initial state \mathbf{q}'_0 and a time increment Δt , the solution of the linearized equation is of the form $\mathbf{q}'(\Delta t) = \mathbf{M}\mathbf{q}'_0$, where $\mathbf{M} = e^{\mathcal{L}\Delta t}$ is the exponential propagator. The eigenvalues $\lambda = \sigma + i\omega$ and the eigenvectors \mathbf{Q} of \mathcal{L} are related to those of \mathbf{M} , namely (Λ, \mathbf{V}) , by the following equations: $\lambda = \frac{\log(\Lambda)}{\Delta t}$, $\mathbf{Q} = \mathbf{V}$. Therefore, one can compute the eigenpairs of \mathbf{M} and easily recover those of \mathcal{L} by the latter equations; the advantage of this procedure is that one does not need to compute \mathcal{L} since the action of the exponential propagator onto a generic vector \mathbf{q}'_0 can be approximated by integrating the linearized Navier–Stokes equations from $t = 0$ to $t = \Delta t$ with initial solution \mathbf{q}'_0 . This allows one to compute Λ and \mathbf{V} by using an efficient Arnoldi iteration. In the present work, we also avoid the linearization of the Navier–Stokes equations by computing numerically the effect of the linear operator employing a perturbation of the solution, namely, $\mathbf{M}\mathbf{q}'_0 \approx [\mathbf{N}(\mathbf{q}_b + \epsilon \mathbf{q}'_0) - \mathbf{N}(\mathbf{q}_b)]/\epsilon$, where \mathbf{N} indicates the integration of the nonlinear Navier–Stokes equations from $t = 0$ to $t = \Delta t$ and ϵ is a small parameter.

3. Results

3.1. Flow configuration and computational model

We consider an axisymmetric jet of fuel into a cylindrical domain filled with oxidizer. The nondimensional flow parameters are set to match exactly the cases studied in [2] and [1]. In this configuration, being the fuel flow rate

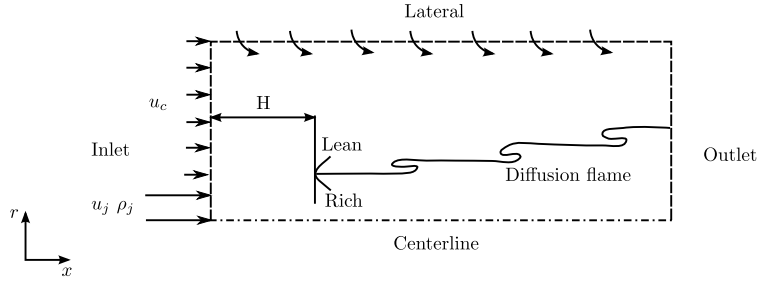


Fig. 1: Scheme of considered test case as proposed in reference [2].

| Da | St | reference [2] | | Present results | | |
|------------------|---------------|---------------|-------|-----------------|-------|-------|
| | | H_s | H_m | St | H_s | H_m |
| $4.0 \cdot 10^5$ | 0.267 | 4.878 | 1.026 | 0.290 | 4.428 | 1.110 |
| $5.0 \cdot 10^5$ | 0.284 | 1.913 | 0.949 | 0.313 | 1.878 | 1.027 |
| $6.0 \cdot 10^5$ | 0.284 | 0.865 | 0.865 | 0.313 | 0.645 | 0.662 |
| $7.0 \cdot 10^5$ | <i>stable</i> | 0.557 | 0.557 | 0.313 | 0.243 | 0.301 |

Table 1: Results of DNS compared to those of [2].

sufficiently large, the flame lifts off the jet nozzle and stabilizes at some distance downstream of the jet exit plane. Moreover, for a large enough density ratio S_1 , it has been shown that the jet contains a pocket of absolute instability in the *premixing zone* at the nozzle exit [6]. This region acts as a "wavemaker", generating perturbations which are convected and amplified downstream [7, 2].

The jet of fuel with velocity u_j and density ρ_j enters through a circular nozzle of diameter d at $x = 0$ and is aligned along the axis of the cylindrical chamber. At the inlet, the jet is surrounded by a co-flow of oxidizer with velocity $u_c = 0.01$.

For validation purpose, we set the nondimensional parameters in the governing equations to the same values employed by [2] and [1], namely: $Re = 1000$, $S_1 = 7$, $S_2 = 6$, $Pr = Sc = 0.7$, $\kappa = 0.01$, $\alpha = 0.833$, $\beta = 3$, $s = 2$ (corresponding to a stoichiometric mixture fraction $Z_{st} = 0.333$). Four values of the Damköhler number have been considered in the present analysis, namely, 4×10^5 , 5×10^5 , 6×10^5 , 7×10^5 .

Concerning inlet boundary condition, Michalke's profile number two [8] has been employed,

$$f(r) = \frac{1}{2} \left\{ 1 + \tanh \left[\frac{1}{4} \frac{d}{2\theta} \left(\frac{d}{2r} - \frac{2r}{d} \right) \right] \right\}, \quad (7)$$

$$u_x(0, r) = (u_j - u_c)f(r) + u_c, \quad Z(0, r) = f(r), \quad T(0, r) = 0, \quad (8)$$

with the ratio of the jet radius $d/2$ to momentum thickness of the shear layer θ equal to $d/2\theta = 12.5$. Moreover, $\partial p / \partial x = 0$ has been imposed at inlet points. At the lateral boundary, $T(r = r_{max}) = 0$, $Z(r = r_{max}) = 0$, and the wall normal derivative of the velocity components and pressure have been set to zero. Finally, along the centreline, axisymmetry is imposed, whereas, at the outlet boundary, convective boundary conditions have been employed for velocity, temperature and mixture fraction, imposing $p = 0$.

We performed firstly a direct numerical simulation (DNS) to analyse the time evolution of the flow and then we applied the selective frequency damping technique (SFD)[9] to compute the base flow for the stability analysis. A modified version of the spectral-element code *Nek5000* [10] has been employed to solve the Navier–Stokes equations and to perform the stability analysis. An Arnoldi iteration has been also implemented to compute the eigenpairs of the exponential propagator \mathbf{M} . The computational domain for the DNS has length equal to 10 in the axial direction (x) and 5 in the radial (r) one [2]. For the spatial discretization, 146 spectral elements have been used in axial direction and 74 elements in radial direction. The Galerkin approximation has been employed. The solution is expanded within the spectral elements using Legendre polynomials of order $N = 12$ at the Gauss–Lobatto–Legendre quadrature points. Concerning the time discretization, a second-order-accurate backward differentiation has been employed [10]. The

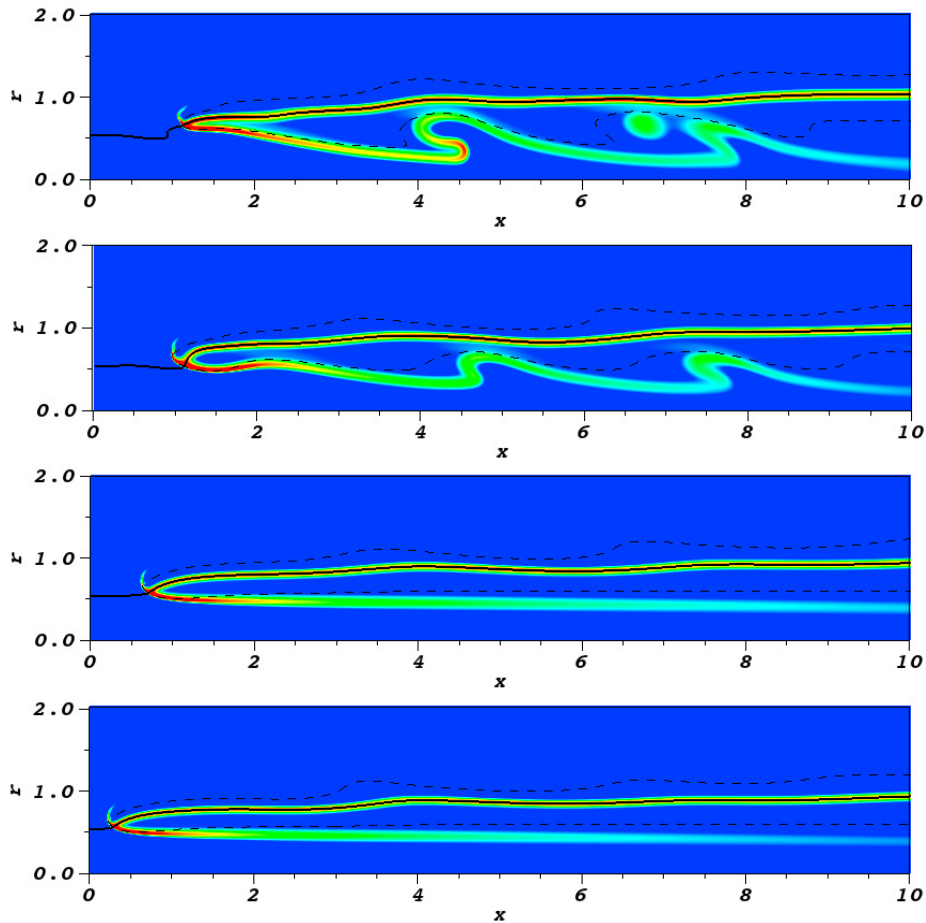


Fig. 2: Snapshots at time $t = 500$ of the lifted flames obtained by four simulations: $Da = 4 \times 10^5, 5 \times 10^5, 6 \times 10^5, 7 \times 10^5$ (top to bottom). Contours of $\ln(\omega)$ (red, -5 , blue -16) are plotted together with the stoichiometric surface (continuous black line) and the temperature contour $T = 0.5$ (dashed black line).

nondimensional time step is equal to 0.001. Both the number of elements in space and the time step have been determined by a refinement study whose details are omitted for brevity.

3.1.1. Discussion of the results

For sufficiently large inlet jet velocity u_j , the flame stabilizes at a lift-off height H defined as the minimum axial distance from the nozzle at which the temperature is $T > 0.5$ for any radius (see figure 1) [2]. This flow configuration originates a typical triple-flame structure characterized by rich and lean premixed branches which anchor a diffusion flame extending downstream along with the stoichiometric surface [11].

Figure 2 provides four snapshots at $t = 500$ showing the contours of the logarithm of the reaction rate for four different values of Da . In all cases, the computations clearly capture the triple-flame structure. One can see also the temperature contour $T = 0.5$ (dashed line) close to the stoichiometric surface and exactly on the triple flame front. When Da is increased, the flame becomes more stable and the lift-off height decreases; for $Da \geq 6 \times 10^5$ a barely unsteady solution is obtained. The time-averaged value of the lift-off height, H_m , is reported in table 1 along with the lift-off height, H_s , obtained by the SFD technique and the Strouhal number, St , computed by an FFT analysis of the H time history. These data are compared with those provided by [2]. For $Da = 4.0 \times 10^5$ and $Da = 5.0 \times 10^5$, after the initial transient, the flame oscillates around a mean value, H_m , that reasonably agrees with the values found by [2]. Whereas, when Da is further increased we obtain lower H_s values with respect to *Nichols et al.*. This is probably due to the different numerical scheme employed. Although the values of the lift-off height do not coincide, we confirm

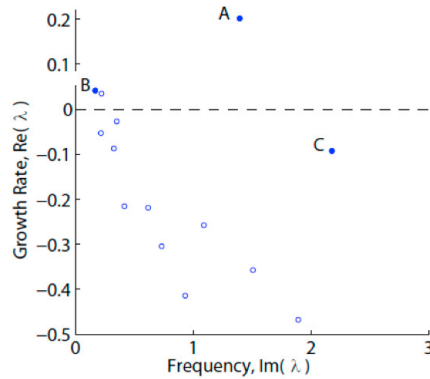


Fig. 3: The least-stable part of the global eigenvalue spectrum (domain M2; $Da = 5 \times 10^5$). Filled circles represent modes A, B and C.

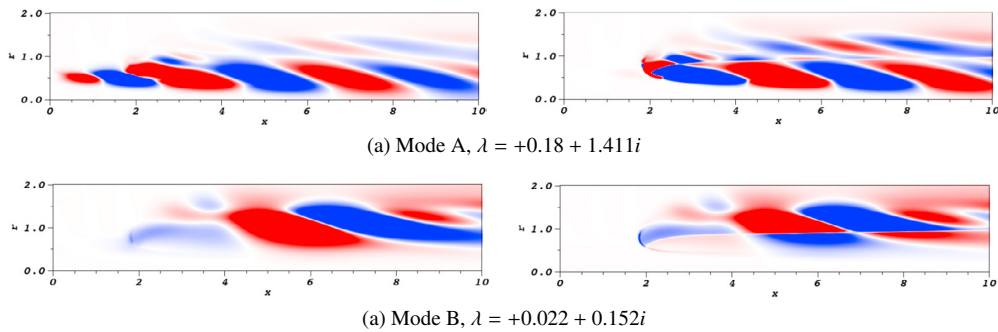


Fig. 4: Real components of global modes A and B for $Da = 5 \times 10^5$. For each mode, the mixture fraction Z (left) and the temperature T (right) are shown.

that the case with $Da = 6 \times 10^5$ can be considered barely unstable with only very small oscillations of the diffusive flame tip.

3.2. Global stability

In order to estimate the influence of the length of the computational domain on the global stability of this problem we employed two domains: M1 with $x_{max} = 10$ and $r_{max} = 5$; and M2 with $x_{max} = 15$ and $r_{max} = 5$. M1 is discretized using 146 spectral elements in axial direction and 74 elements in radial direction, whereas domain M2 has 219 and 74 elements, respectively. This choice allows a direct comparison with the same computational domains employed in reference [1] for the case with $Da = 5 \times 10^5$.

In the related spectrum, see figure 3, among the well-converged modes, we find an isolated unstable high-frequency mode, labelled mode A, and a branch of low-frequency modes very close to the marginally stable condition ($Re(\lambda) = 0$); such a branch is composed of free-stream vortical modes and only the most unstable of them, labelled mode B, will be shown in detail. Finally, we have also found another isolated stable high-frequency mode, labelled mode C.

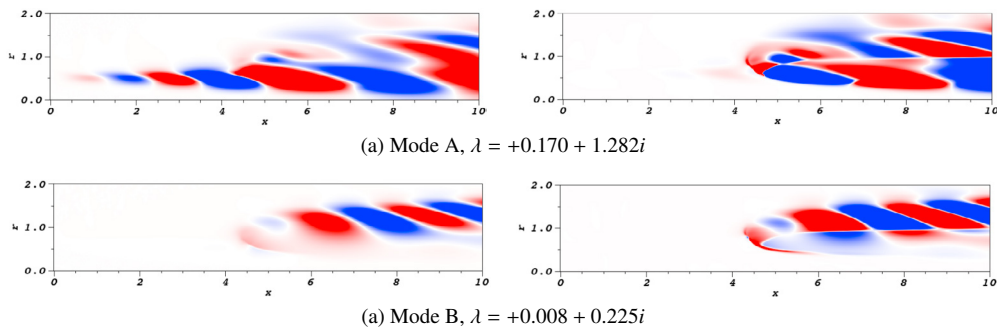
Table 2 provides the eigenvalues associated to these modes computed using domain M1 and M2, compared with the results of [1]. It's worth remarking that the present global stability analysis can be very sensitive to the domain dimensions. In fact, small discrepancies in the real and imaginary part of the eigenvalues computed using domains M1 and M2 can be observed in table 2. However, these discrepancies do not change the stability behavior of the three analyzed modes. The results agree reasonably well with those provided in [1], even if, using domain M2, these authors find that mode B is (barely) stable. Also the frequencies of the modes agree very well and the shape of the spectrum is very similar. Considering the results obtained using domain M1, mode A has growth rate $Re(\lambda) = 0.18$ with pulse $Im(\lambda) = 1.411$. The corresponding real components, given in figure 4a, show that this mode shape is dominant in the premixing zone, between the inlet and the flame base. In fact mode A is linked to the pocket of instability upstream of

| | [1] | | Computed | |
|--------|------------------|-------------------|-------------------|-------------------|
| | M1 | M2 | M1 | M2 |
| Mode A | $0.157 + 1.363i$ | $0.157 + 1.365i$ | $0.180 + 1.411i$ | $0.200 + 1.382i$ |
| Mode B | $0.020 + 0.172i$ | $-0.005 + 0.170i$ | $0.022 + 0.152i$ | $0.041 + 0.167i$ |
| Mode C | — — — — — | — — — — — | $-0.128 + 2.159i$ | $-0.093 + 2.174i$ |

Table 2: Eigenvalues computed for $Da = 5 \times 10^5$ using domains M1 and M2.

| Da | Mode A | Mode B | Mode C |
|-------------------|-------------------|-------------------|-------------------|
| 4.0×10^5 | $+0.170 + 1.282i$ | $+0.008 + 0.225i$ | $-0.084 + 2.025i$ |
| 7.0×10^5 | $-0.487 + 2.183i$ | $+0.037 + 0.203i$ | $-0.572 + 2.812i$ |

Table 3: Eigenvalues computed using domain M1.

Fig. 5: Real components of global modes A and B for $Da = 4 \times 10^5$. For each mode, the mixture fraction Z (left) and the temperature T (right) are shown.

the flame base. Mode B has growth rate $Re(\lambda) = 0.0222$ with pulse $Im(\lambda) = 0.1518$. Figure 4b shows that in this case the mode is localized further downstream, along the outer part of the flame and grows radially away from the axis of the jet. Finally, mode C has $Re(\lambda) = -0.128$ with pulse $Im(\lambda) = 2.159$. It is located near the stability limit and its shape (not shown) is very similar to mode A (related to the premixed zone) with higher frequency. Mode C was found also by [1] but it was not analyzed.

Table 3 and figures 5 and 6 provide the results obtained with $Da = 4 \times 10^5$ and $Da = 7 \times 10^5$ employing domain M1, for completeness.

For $Da = 7 \times 10^5$, mode A becomes stable. On the other hand, mode B remains unstable with a frequency almost unchanged. This oscillation characterizes the diffusive tip of the flame, as indicated by the corresponding eigenvector. Finally, mode C becomes more stable and its frequency further increases.

For the case with $Da = 4 \times 10^5$, the results show that mode A is still the most unstable mode, with growth rate smaller than that found for the case with $Da = 5 \times 10^5$. Finally, other two unstable modes appear with the same shape of mode A (not shown).

4. Conclusions

In this work, a numerical method based on the time-stepper approach proposed by Edwards et al. (1994) and Bagheri et al. (2009) has been combined with a numerical linearization of the governing equations and employed to study the global stability of reacting flows. This method allows one to analyze the stability of diffusion flames without the direct evaluation and storage of the linearized operator; in this way, a remarkable reduction of the storage capacity is achieved, which renders the method suitable for three dimensional flow computations. Furthermore, a

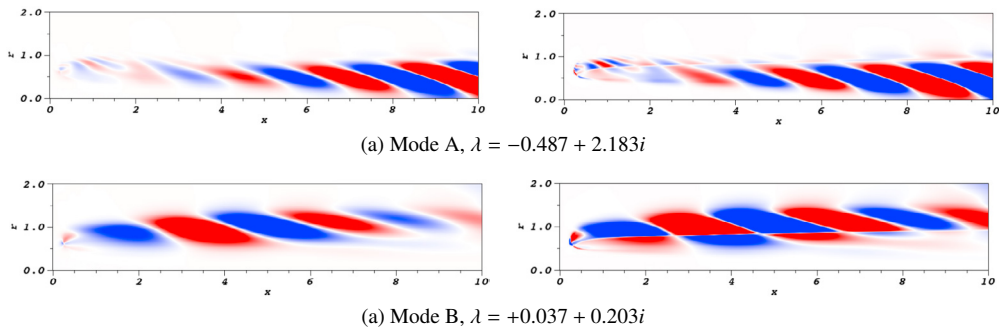


Fig. 6: Real components of global modes A and B for $Da = 7 \times 10^5$. For each mode, the mixture fraction Z (left) and the temperature T (right) are shown.

more flexible approach is obtained, which can be applied straightforwardly to any complex system of conservation equations governing the dynamics of a reacting flows.

The method has been successfully validated versus the results of Qadri et al. (2015) using the same test case proposed by Nichols (2008) concerning a jet diffusion flame.

We have confirmed the results of Qadri et al. (2015); namely, we have found two modes responsible of the oscillation of the flame, labelled mode A and mode B. Mode A is associated with the upstream global unstable region and is linked to high frequency oscillations. Instead mode B is responsible of the low frequency oscillations initially found by Nichols et al. (2008) and is located in the outer part of the flame. In conclusion, the proposed method represents a valid alternative to the classical linearization approach for studying the global stability of complex three-dimensional reacting flows, requiring a very small storage capacity.

References

- [1] U. A. Qadri, G. J. Chandler, M. P. Juniper, Self-sustained Hydrodynamic Oscillations in Lifted Jet Diffusion flames: Origin and Control, *Journal of Fluid Mechanics*, (CUP), vol. 775 (2015) 201–222.
- [2] J. Nichols, P. Schmid, The Effect of a Lifted flame on the Stability of Round Fuel Jets, *Journal of Fluid Mechanics*, (CUP), vol. 609, pp 275–284 (2008) 275–284.
- [3] S. Bagheri, A. E. L. Brandt, D. S. Henningson, Matrix-free methods for the stability and control of boundary layers, *AIAA Journal* 47 (5) (2009) 1057–1068.
- [4] W. S. Edwards, L. S. Tuckerman, R. A. Friesner, D. C. Sorenson, Krylov methods for the incompressible navier-stokes equations, *Journal of computational physics* 110 (1994) 82–102.
- [5] N. Peters, Combustion theory, RWTH Aachen university, CEFRC Summer School Princeton.
- [6] J. Nichols, P. Schmid, J. J. Riley, Self-sustained Oscillations in Variable Density Round Jets, *Journal of Fluid Mechanics*, (CUP), vol. 582 (2007) 341–376.
- [7] J.-M. Chomaz, Global Instabilities in spatially developing flows: non normality and non linearity, *Annu. Rev. Fluid Mechanics*, 37 (2007) 357–392.
- [8] A. Michalke, Survey on Jet Instability Theory, *Prog. Aerospace Sci*, 21 (1984) 159–199.
- [9] E. Åkervik, L. Brandt, D. S. Henningson, J. Høpfner, O. Marxen, P. Schlatter, Steady Solutions of the Navier-Stokes equations by Selective Frequency Damping, *Physics of Fluids*, 18 (2006) 068102.
- [10] P. Fischer, J. Lottes, S. Kerkemeir, nek5000 Web pages, <http://nek5000.mcs.anl.gov> (2008).
- [11] S. Ghosal, L. Vervisch, Theoretical and Numerical study of Symmetrical Triple Flame using the parabolic flame approximation, *Annu. Rev. Fluid Mechanics*, 37 (2000) 357–392.